

## GALACTIC STRUCTURE FROM THE *SPACELAB* INFRARED TELESCOPE. II. LUMINOSITY MODELS OF THE MILKY WAY

S. M. KENT,<sup>1</sup> T. M. DAME, AND G. FAZIO

Harvard-Smithsonian Center for Astrophysics, Mail Stop 20, 60 Garden Street, Cambridge, MA 02138

*Received 1990 December 3; accepted 1991 March 13*

### ABSTRACT

The three-dimensional luminosity distribution of the Milky Way has been determined from a  $2.4\ \mu\text{m}$  map of the northern Galactic plane. The radial surface brightness profile of the disk has an exponential scale length of 3.0 kpc (assuming  $R_0 = 8$  kpc). The vertical distribution of light follows the law  $\exp(-|z|/h_z)$  more closely than a canonical  $\text{sech}^2$  profile. In the solar neighborhood, the scale height  $h_z$  is  $\sim 247$  pc (assuming  $R_0 = 8$  kpc), in agreement with star counts perpendicular to the Galactic plane. The scale height is not constant with radius but decreases to  $\sim 165$  pc at  $R = 5$  kpc. To first order, the bulge can be represented by an oblate spheroid with an axis ratio  $b/a = 0.61$  and again, an exponential luminosity profile. The  $2.2\ \mu\text{m}/12\ \mu\text{m}$  flux ratio for the bulge is typical of other dust-free spheroidal systems.

Luminosity fluctuations along the galactic plane are found to be caused chiefly by variations in the line-of-sight extinction. These fluctuations can be reproduced quantitatively by a detailed model for the dust distribution and allow an approximate calibration of the dust/gas ratio in regions of high (10 mag at  $V$ ) optical depth.

*Subject headings:* galaxies: structure — galaxies: The Galaxy — infrared: sources — interstellar: matter

### 1. INTRODUCTION

The Infrared Telescope (IRT), flown aboard the Space Shuttle during 1985 as part of the *Spacelab 2* mission, scanned a large fraction of the sky in several infrared bands with a spatial resolution of  $\sim 1^\circ$ . Details of the instrument and experiment may be found in Koch et al. (1982) and Melnick et al. (1987). Data from the shortest wavelength band, centered at  $2.4\ \mu\text{m}$  with a bandpass of  $1.3\ \mu\text{m}$ , were used to produce maps of the Galactic plane between longitudes  $340^\circ$  to  $120^\circ$  and latitudes  $-30^\circ$  to  $+30^\circ$ . The data and calibration procedures were presented in Kent et al. (1991, hereafter Paper I). For convenience, all intensities have been color corrected to the standard infrared  $K$  band centered at  $2.2\ \mu\text{m}$  assuming that the galaxy spectrum has the form  $f_\lambda \propto \lambda^{-2.5}$ .

In this paper we derive a model for the three-dimensional luminosity distribution in the Milky Way based on those data. The Galaxy is modeled conventionally as a spheroidal bulge and a thin disk with an exponential radial surface brightness profile. The data allow us to determine the luminosity profile of the bulge, the radial exponential scale length of the disk, and the shape of the vertical distribution of light in the disk. They do not allow us to distinguish the details of thick versus thin disk (e.g., Gilmore & Reid 1983) or the luminosity profile of the outer spheroid of the Galaxy.

Numerous models have been constructed for the luminosity distribution within the Milky Way (e.g., de Vaucouleurs & Pence 1978; Bahcall & Soneira 1980; Caldwell & Ostriker 1981). Because the luminosity distribution of the Milky Way cannot be determined directly (at least from optical observations), the models incorporate components which are chosen to have forms representative of other spiral galaxies. Scale parameters are usually derived by indirect means, e.g., from local observations of the solar neighborhood and by comparison with the properties of external galaxies.

The  $2.4\ \mu\text{m}$  band is much better than the optical for direct observations of Galactic structure: interstellar extinction is reduced by more than a factor of 10, yet the wavelength is short enough that thermal emission from dust is still negligible. Zodiacal light is also minimal. The principal source of emission is old-disk K and M giants, with only minor contributions from young M supergiants, at least locally (Jones et al. 1981; Ishida & Mikami 1982). Extinction due to dust is still not negligible, however, and so any model to reproduce the observed  $2.4\ \mu\text{m}$  emissivity must also incorporate an accurate model of the dust distribution.

The Galactic plane has been observed extensively at  $2.4\ \mu\text{m}$  from several experiments using balloon-borne infrared telescopes by two groups, one at Nagoya University (e.g., Ito, Matsumoto, & Uyama 1976; Hayakawa et al. 1977, 1981) and one at Kyoto University (e.g., Maihara et al. 1978; Oda et al. 1979). The observations were made through a narrow filter at a wavelength of  $2.4\ \mu\text{m}$ , making use of a window in the OH airglow spectrum. The spatial resolution in the different experiments ranged from  $0.6$  to  $3^\circ$ . All together, these experiments cover the range  $-70^\circ < l < 75^\circ$ ,  $-5^\circ < b < 5^\circ$ , except extending to  $-10^\circ < b < 10^\circ$  in the bulge region. These data have been fitted with various models (Hayakawa et al. 1977, 1981; Oda 1985) for the emissivity which incorporate bulge, disk, and ring components. In all cases, the disk was modeled as an oblate spheroid of constant ellipticity rather than a more conventional exponential disk with an independent vertical luminosity profile. Unfortunately, the full data in those papers is presented only in the form of contour plots which cannot be used easily for further analysis. The present paper differs from that work in two ways: first, a conventional disk model is used, and second, the model is fitted out to a Galactic latitude of  $\pm 10^\circ$ . Only data from the north Galactic hemisphere are used.

The paper is organized as follows. Section 2 presents a description of the luminosity and dust models used. Section 3 gives the results of various fits of these models to the observed  $2.4\ \mu\text{m}$  data of Paper I. Section 4 gives a more detailed model for the light distribution in the range  $10^\circ < l < 60^\circ$  in which

<sup>1</sup> Presidential Young Investigator.

the modulation of the  $2.4\ \mu\text{m}$  light profile is shown to arise almost entirely from variations in extinction along the line of sight. Section 5 compares our results with previous work on Galactic structure. Section 6 compares our  $2.4\ \mu\text{m}$  view of the bulge with that of *IRAS*. Conclusions are summarized in § 7. Throughout, we take the Sun to be at a distance  $R_0 = 8\ \text{kpc}$  from the Galactic center, which is a compromise amongst recent determinations (Reid 1989); physical quantities taken from other sources have been corrected to this distance where necessary. All distance scale as  $R_0$ , luminosities as  $R_0^2$ , and luminosity space densities as  $R_0^{-1}$ , while all surface brightnesses are independent of  $R_0$ .

## 2. LUMINOSITY AND DUST MODELS

The Galaxy is modeled with disk and bulge components as follows. The disk is assumed to have the form:

$$v(r, z) = \mu_D e^{-r/h_r} g(z/h_z)/h_z, \quad (1)$$

where  $(r, z)$  are cylindrical coordinates,  $v$  is the space emissivity,  $\mu_D$  is the vertically integrated central surface brightness,  $h_r$  is a constant scale length,  $h_z$  is a vertical scale height that may be a function of  $r$ , and the function  $g$  is normalized such that  $\int_{-\infty}^{\infty} g(x) dx = 1$ . Two functions have been used for the vertical distribution:

$$g(x) = \frac{1}{4} \text{sech}^2(x/2), \quad (2)$$

$$g(x) = \frac{1}{2} \exp(-|x|). \quad (3)$$

The former corresponds to the vertical density profile of a self-gravitating isothermal sheet and was proposed by van der Kruit & Searle (1981) as providing a good match to the observed light profiles perpendicular to galactic disks in edge-on galaxies. The factor 2 is included so that at large  $x$  the profile becomes  $\exp(-|x|)$ . However, Pritchett (1983) found that a pure exponential provides a better fit to star count data in the Milky Way than a  $\text{sech}^2$  law. Wainscoat, Freeman, & Hyland (1989) found from IR photometry of the edge-on galaxy IC 2531 that the perpendicular light profile is more peaked in the plane than a  $\text{sech}^2$  profile, and they also suggested that a pure exponential provides a better description. Van der Kruit (1988) reinvestigated the situation for the Milky Way and argued that a  $\text{sech}^2$  profile, which is of an intermediate form, works best. The Bahcall & Soneira (1980) and Jones et al. (1981) models assume an exponential law (albeit with different scale lengths for stars of different luminosity). Both the exponential and  $\text{sech}^2$  profiles will be tried here. In a real disk with a mix of stars of different kinematics, neither profile can be expected to provide a perfect representation of any single or combination of populations, and so they should be looked upon more as convenient approximations to the true vertical distribution. Nominal values for the scale lengths are  $h_r = 3500\ \text{pc}$  (de Vaucouleurs & Pence 1978) and  $h_z = 230\text{--}250\ \text{pc}$ . This latter value is the approximate vertical  $e$ -folding length for the total  $K$ -band luminosity in the multicomponent model of Jones et al. (1981) and Garwood & Jones (1987). We note that Bahcall & Soneira (1980) also use a scale height  $250\ \text{pc}$  for giant stars, which are expected to dominate the  $2.2\ \mu\text{m}$  light.

de Vaucouleurs & Pence (1978) modeled the Milky Way spheroid with a single  $r^{1/4}$  law. However, an extrapolation of that law into the bulge region provides a poor fit to the minor axis profile (Fig. 1). Instead, as Fig. 1 shows, inside a radius of  $10^\circ$ , the bulge profile can be fitted much better with an exponential profile with a scale length of  $2.7$  or  $378\ \text{pc}$ . In fact,

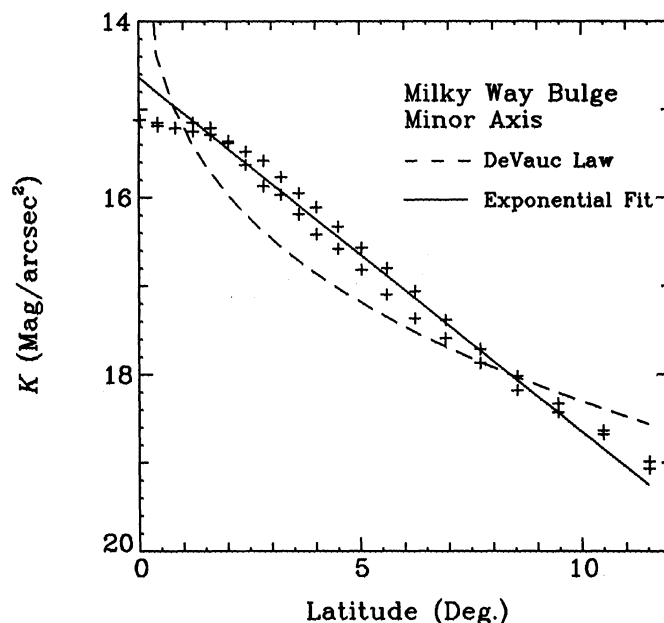


FIG. 1.—Bulge minor-axis profile, show both an exponential fit and the profile predicted by the spheroid model of de Vaucouleurs & Pence (1978); the latter profile assumes  $V-K = 3.2$ .

popular wisdom to the contrary, there is no reason to believe that the inner bulge and outer spheroid of the Milky Way can be fitted with one single component. In NGC 4565, an edge-on galaxy that is quite similar to the Milky Way, Kormendy's (1980) minor axis profile shows that the bulge+spheroid in that galaxy cannot be matched by any single standard fitting function. Frankston & Schild (1976) found that the inner bulge of NGC 4565 is fitted best with an exponential profile, but outside a distance of  $50''$ , Kormendy's profile flattens out to a power-law shape. We do not attempt to include an extra "spheroid" component as it would likely contribute relatively little light at low Galactic latitudes. The Milky Way bulge isophotes are more boxy than ellipses (Paper I, Fig. 5), a common situation for low-luminosity bulges (e.g., Jarvis 1986). Consequently the bulge is modeled as a modified spheroid with density profile

$$v(s) = (\mu_0/\pi h_B) K_0 (s/h_B), \quad (4)$$

where  $v$  is the space luminosity density,  $\mu_0$  is the projected central surface brightness,  $h_B$  is the major-axis scale length,  $\epsilon_B$  is the bulge ellipticity, and  $K_0$  is a modified Bessel function. The radial coordinate  $s$  is given by  $s^4 = R^4 + [Z/(1 - \epsilon_B)]^4$ , a form which has a "boxy" appearance in projection. We stress that this bulge model is intended to match only the bulge region between  $1^\circ$  and  $10^\circ$  and not the extended spheroid or the central cusp in the Galactic Center (Becklin & Neugebauer 1968).

There is a prominent "hump" of emission in the range  $10^\circ < l < 35^\circ$ ,  $-1^\circ < b < 1^\circ$  which requires an extra component besides the exponential disk. We have chosen not to model the hump here and will ignore data in that region from our fits, although we will return to this region in § 4. Hayakawa et al. (1977) were able to reproduce the hump successfully using an ad hoc ring model; however, the data of Hayakawa et al. (1981) show that the hump is not repeated symmetrically in the

southern hemisphere, so this feature may be caused by a spiral arm rather than an axisymmetric ring.

For the purposes of modeling the global luminosity distribution, we use a simple model for the dust distribution. We assume that the dust/hydrogen ratio in the interstellar medium is a constant and depends on only the total density of hydrogen atoms, whether atomic or molecular. The calibration is as follows. We use  $A_{2.4\mu\text{m}} = A_V/14$ ,  $A_V = 3E(B-V)$ , and  $E(B-V) = N(H_{20})/58$  (Bohlin, Savage, & Drake 1978), where  $E(B-V)$  is the  $B-V$  color excess and  $N(H_{20})$  is the hydrogen atom column density in units of  $10^{20} \text{ cm}^{-2}$ . Our value for  $A_{2.4\mu\text{m}}/A_V$  comes from taking Rieke & Lebofsky's (1985) value of  $A_{2.4\mu\text{m}}/A_V = 1/10.2$  and reducing it by a factor of 1.4 to allow for clumpiness in the molecular gas (Hayakawa et al. 1981). We will show in § 4 that our calibration is likely close to the correct value.

The atomic and molecular hydrogen distributions are modeled independently. For the atomic hydrogen, we assume that the  $\text{H I}$  is distributed axisymmetrically in the Galaxy with a Gaussian vertical distribution that has an FWHM of 200 pc, which is an average of values found by Baker & Burton (1975) and Lockman (1984). The radial surface density profile is taken from Burton (1988). The molecular hydrogen, as traced by CO emission, is also assumed to be distributed axisymmetrically in the Galaxy with a Gaussian vertical distribution that has an FWHM of 112 pc (Bronfman et al. 1988). The radial distribution of CO is different between the northern and southern hemispheres; only northern hemisphere data is used here. The density profile comes from Bronfman et al. (1988), Dame et al. (1987), and Grabelsky et al. (1987). The scaling from CO intensity to  $\text{H}_2$  density is done using a conversion factor of  $N(\text{H}_2)/W_{\text{CO}} = 2.3 \times 10^{20} \text{ cm}^{-2}/(\text{K km s}^{-1})$  (Strong et al. 1988).

### 3. MILKY WAY PARAMETERS

Given a set of scale parameters for the luminosity model, we compute the projected surface brightness at the solar position by a numerical integration of the model along a given line of sight. For comparison with the observations of Paper I, we average the surface brightness profiles into four cuts of constant latitude parallel to the Galactic equator covering the ranges  $|b| < 1^\circ$ ,  $1^\circ < |b| < 2^\circ$ ,  $2^\circ < |b| < 5^\circ$ , and  $5^\circ < |b| < 10^\circ$ . In fitting the data, we exclude data within  $4^\circ$  of the Galactic center (where the dust model is inadequate), the range  $10^\circ < l < 35^\circ$  in the  $|b| < 1^\circ$  cut, where there is a pronounced excess of light that the model will be unable to reproduce, and a few points that were severely contaminated by bright stars. Because of problems with background variation in the IRT experiment, the data given in Paper I had their zero point adjusted to give 0 intensity at  $l = 66^\circ$ ,  $b = -21^\circ$ . The theoretical models have been adjusted in the same fashion. The dominant "statistical" error arises from fluctuations due to the presence of discrete stars and small-scale fluctuations in extinction. The dominant systematic error comes from the two sources: first, all data points potentially can still have an error corresponding to a surface brightness of  $20 \text{ mag arcsec}^{-2}$ , and second, the Galaxy may not be adequately represented by the model. Somewhat arbitrarily, we give all points equal weight in the fit.

First we tried an entirely standard model of the Galaxy: a radial scale length  $h_R = 3.5 \text{ kpc}$ ,  $h_z = 250 \text{ pc}$ , and a  $\text{sech}^2$  vertical profile. The bulge scale length on the minor axis was fixed at  $h_b = 378 \text{ pc}$ . The ellipticity was taken to be  $\epsilon = 0.35$ . The

best fit is shown in Figure 2. The vertical normalization has been chosen to best match the  $2^\circ$ – $5^\circ$  cut. Clearly, the model fails miserably in the Galactic plane, predicting way too little light as compared with the higher latitudes.

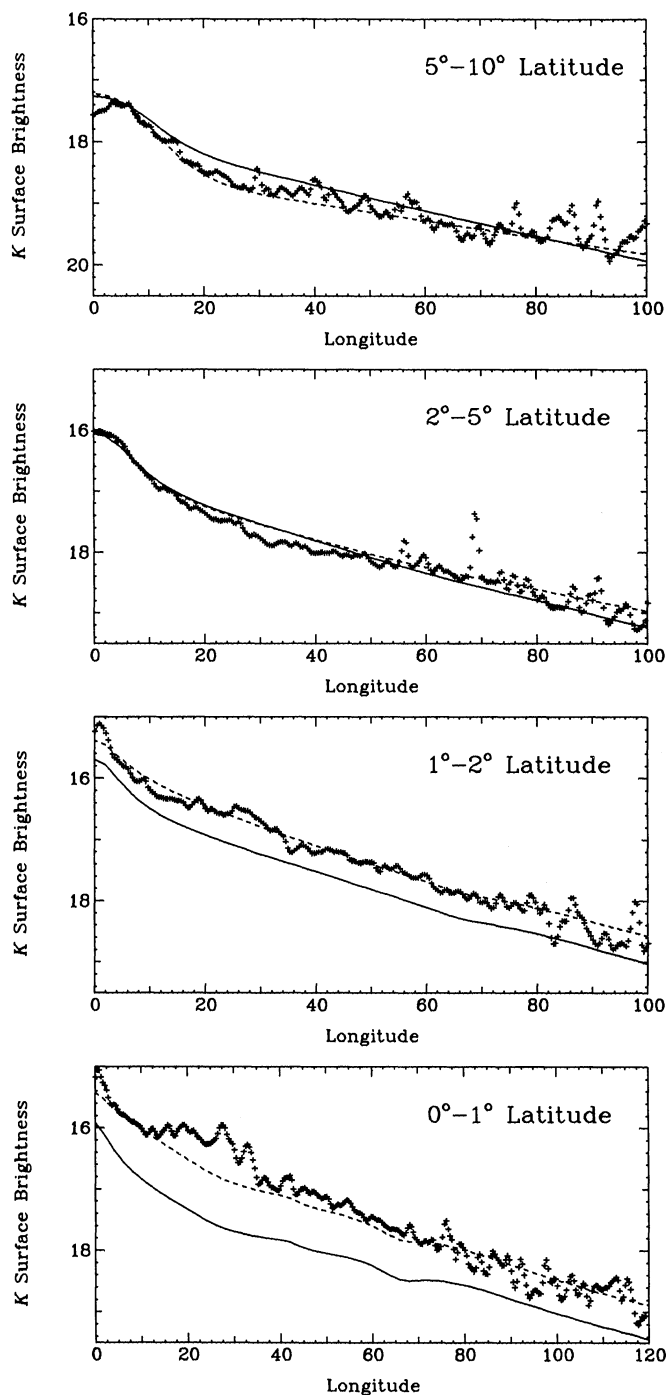


FIG. 2.—Two fits to the longitudinal surface brightness profiles of the  $2.4 \mu\text{m}$  flux expressed in K-band  $\text{mag arcsec}^{-2}$ . The different latitude bands are an average of both sides of the Galactic plane. Longitudes are expressed in degrees. Both models have a  $\text{sech}^2$  vertical density profile. The solid line shows a model using standard values for the Milky Way structure parameters. The dashed line shows a model in which the parameter values were adjusted by a least-squares fit.



TABLE 1  
MILKY WAY MODEL PARAMETERS

Parameter	Value, $\pm 1 \sigma$ Error	Units
Sech <sup>2</sup> Vertical Profile		
Disk: $\mu_D$ .....	$1072 \pm 214$	$L_\odot \text{ pc}^{-2}$
$h_R$ .....	$2775 \pm 499$	pc
$h_z$ .....	$121 \pm 34$	pc
Bulge: $\mu_B$ .....	$6208 \pm 1241$	$L_\odot \text{ pc}^{-2}$
$h_B$ .....	$634 \pm 222$	pc
$\epsilon_B$ .....	$0.26 \pm 0.18$	pc
Exponential Vertical Profile		
Disk: $\mu_D$ .....	$1208 \pm 242$	$L_\odot \text{ pc}^{-2}$
$h_R$ .....	$2694 \pm 485$	pc
$h_z$ .....	$204 \pm 57$	pc
Bulge: $\mu_B$ .....	$7710 \pm 1542$	$L_\odot \text{ pc}^{-2}$
$h_B$ .....	$500 \pm 175$	pc
$\epsilon_B$ .....	$0.19 \pm 0.18$	pc
Exponential Vertical Profile; Variable $h_z$		
Disk: $\mu_D$ .....	$978 \pm 196$	$L_\odot \text{ pc}^{-2}$
$h_R$ .....	$3001 \pm 540$	pc
$h_{\min}$ .....	165	pc
$R_{\min}$ .....	$5300 \pm 2650$	pc
$h_z(R_\odot)$ .....	$247 \pm 69$	pc
Bulge: $\mu_B$ .....	$7395 \pm 1479$	$L_\odot \text{ pc}^{-2}$
$h_B$ .....	$667 \pm 233$	pc
$\epsilon_B$ .....	$0.39 \pm 0.18$	pc

Next, we made a least-squares fit to the data, adjusting three disk parameters ( $\mu_D$ ,  $h_R$ , and  $h_z$ ) and three bulge parameters ( $\mu_B$ ,  $h_B$ , and  $\epsilon_B$ ). The resulting fit is also shown in Figure 2, and the model parameters are tabulated in Table 1. Aside from the stretches of data omitted above, the fit is much improved, except that the  $0^\circ$ – $1^\circ$  band is still not entirely satisfactory. Much more disturbing, however, is the fact that the vertical scale height of 122 pc is over a factor of 2 smaller than the expected value.

We then tried replacing the sech<sup>2</sup> vertical profile with an exponential law. The resulting model fit is not shown but is virtually the same as for the sech<sup>2</sup> law. The scale height is now 204 pc, still on the low side compared with what is expected for the solar neighborhood, although the formal error (57 pc) is large. As a final step, we tried models in which the vertical scale height also varies with radius. We tried several possible forms for the scale height variation and finally settled on a model in which the scale height is constant at a value  $h_{\min}$  inside a characteristic radius  $R_{\min}$ , and then increases linearly with radius outside. The two parameters  $h_{\min}$  and  $R_{\min}$  replace the single parameter  $h_z$ . This fit is shown in Figure 3. The improvement over the models with a fixed scale height is significant, although not dramatic. However, the scale height in the solar neighborhood is now 247 pc—very close to the expected value. We shall refer to this final model as the standard model. Parameters for the various sets of models are given in Table 1.

The errors in the parameters include estimates of the contributions from random and systematic errors in the data and from uncertainties in the dust model. The contributions from systematic errors were determined by assuming that the rms error is 60% of the maximum expected error and that systematic errors are correlated over regions  $40^\circ$  in size. To find out

how uncertainties in the dust model affect the fits, we ran two models with the overall dust extinction increased and decreased by a factor 1.25. We assume that the resulting changes in the parameters are  $1 \sigma$  changes. These error estimates may be unduly pessimistic. Not included is a zero-point uncertainty of  $\sim 15\%$  in the flux scale which exists for reasons explained in Paper I. It should be emphasized that many of the parameter errors are highly correlated, so derived quantities

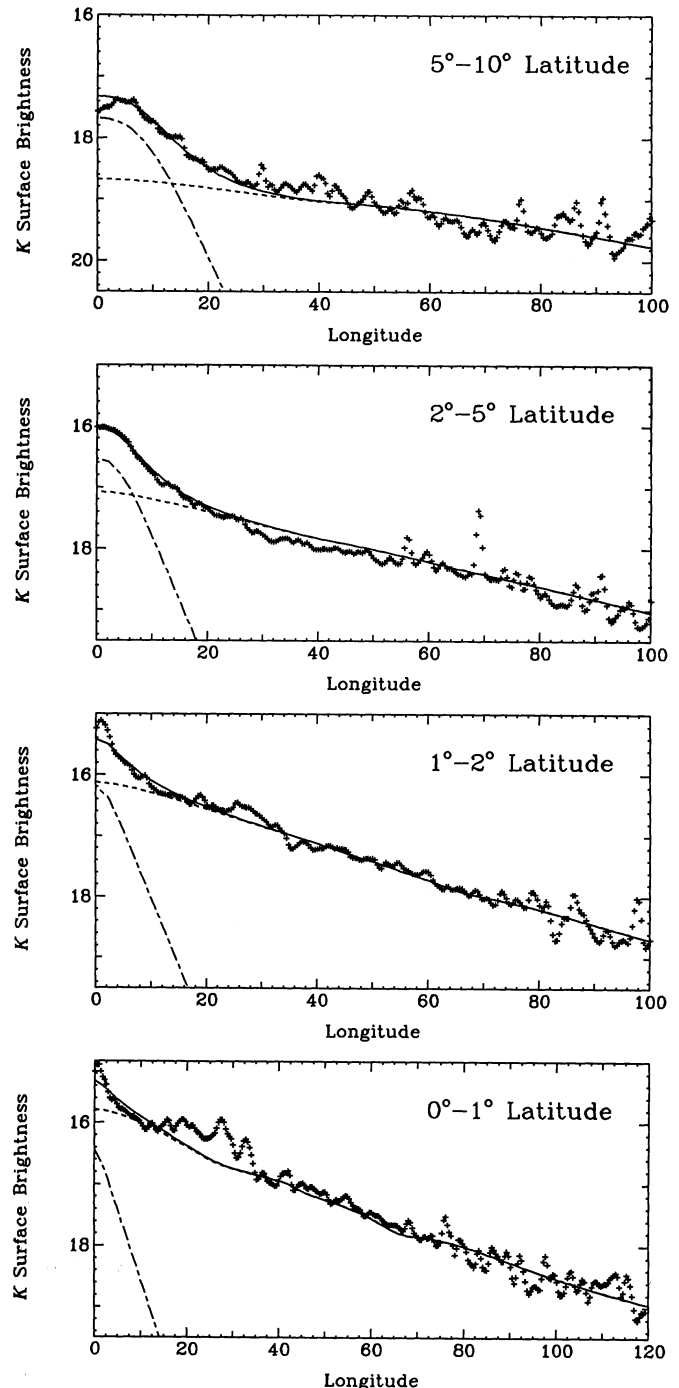


FIG. 3.—Same as Fig. 2, but showing the best-fitting model with an exponential vertical density profile and a variable scale height. The separate bulge and disk components are also shown.

such as total luminosities are better determined than might appear otherwise.

The bulge model is not entirely satisfactory. The predicted minor-axis scale length is 407 pc, considerably larger than the apparent scale length of 378 pc derived from a direct fit to the minor-axis profile. The reason for the discrepancy can be seen in Figure 3. In the top panel showing the  $5^\circ$ – $10^\circ$  latitude cut, the observed profile has a slight depression at  $l = 0^\circ$  which is not allowed for even by our model with box-shaped contours. It is not obvious from our data if the depression is real or an artifact; however, a visual inspection of the recently published *COBE* picture of the Galactic plane (see, e.g., Schwarzschild 1990) seems to show the same feature. In any case, a more accurate bulge model will require allowing for both the ellipticity and isodensity surface shapes to vary with radius.

Taking an absolute  $K$  magnitude for the Sun of 3.41, we find that the total disk luminosity is  $5.5 \times 10^{10} L_\odot$  and the bulge luminosity is  $1.2 \times 10^{10} L_\odot$ . The model predicts a  $2.2 \mu\text{m}$  volume emissivity in the solar neighborhood of  $2.8 \times 10^{24} \text{ W } \mu\text{m}^{-1} \text{ pc}^{-3}$  and a surface flux density of  $1.4 \times 10^{27} \text{ W } \mu\text{m}^{-1} \text{ pc}^{-2}$  (the latter being independent of the assumed  $R_0$ ). From direct star counts, Ishida & Mikami (1982) find values for these parameters of  $3 \times 10^{24}$  and  $2.2 \times 10^{27}$ , respectively, with errors of  $\sim 10\%$ . The former is in excellent agreement with the model; the latter is in only fair agreement and indicates that the mean scale height in Ishida & Mikami's model is larger than that used here. Yet another comparison can be made with the model of Garwood & Jones (1987), which predicts values for these parameters of  $2.3 \times 10^{24}$  and  $1.1 \times 10^{27}$ , respectively. Both are lower by  $\sim 22\%$  than those of our disk model.

#### 4. A CALIBRATION OF THE DUST/GAS RATIO

The surface brightness profile along the Galactic equator,  $|b| < 1^\circ$ , in Figures 2 and 3 appears to show several discrete sources superposed on a smoother background. Melnick et al. (1987) and Hayakawa et al. (1981) have suggested that they may correspond to H II regions and spiral arms, while Okuda (1981) has pointed out that the "sources" are anticorrelated with the CO emission, and thus they may be directions of low extinction. We have tried modeling the latter effect and find that, in fact, the extinction variations are dominant. Because of this we are able to test the calibration of the dust/gas ratio by trying to match the amplitude of the intensity fluctuations.

To reproduce the intensity fluctuations in the 1st quadrant of the  $2.4 \mu\text{m}$  map, we have developed a model for the luminosity and dust distribution inside  $R_0$  that is more detailed than the simple models used in § 3. Following Hayakawa et al. (1977), the luminosity distribution is modeled as the sum of a "thick" disk with parameters derived in § 3 plus a second "thin" disk (actually a ring) of emission. The thin disk is introduced to reproduce the excess of emission in the range  $10^\circ < l < 35^\circ$ . Its spatial distribution is similar to that of the molecular gas, with a Gaussian  $z$  thickness of 112 pc, a peak at 3.7 kpc, a Gaussian falloff toward lower radius, and an exponential falloff toward higher radius. These functional forms and parameters were selected to best reproduce the average intensity in the first quadrant. This thin disk may be a population of young stars associated with the strong concentration of molecular clouds that peak at  $\sim 4.2$  kpc. A plot of the radial distribution of the face-on disk intensity is shown in Figure 4.

The CO survey of Dame et al. (1987) and the 21 cm survey of Weaver & Williams (1973) have been used to derive a three-

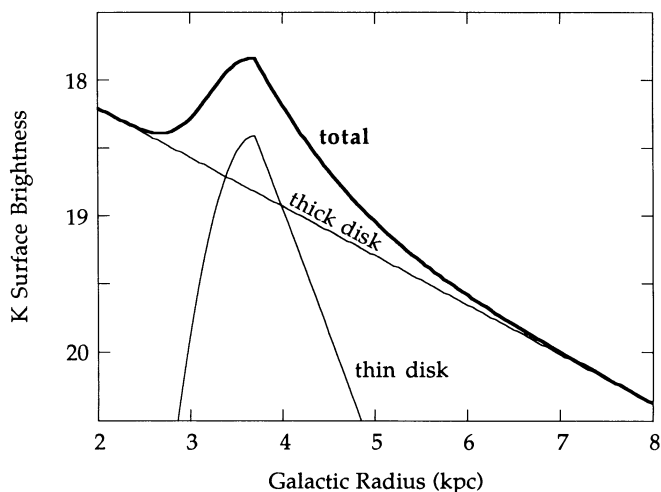


FIG. 4.—Radial profiles of the thick and thin disk components used in the detailed model of the inner Galaxy.

dimensional map of the gas distribution. Briefly, gas distances are derived by combining the observed radial velocities with a model for Galactic rotation. Kinematic distances have a two-fold ambiguity corresponding to a "near" and "far" side of the Galaxy. All emission at  $|b| < 1.5^\circ$  and with a velocity within  $15 \text{ km s}^{-1}$  of the terminal velocity at any longitude is derived equally between the near and far sides. The remaining emission is assigned entirely to the near side because at the  $0.5^\circ$  angular resolution of this analysis, the far side material makes very little contribution. The CO and H I emissivities are converted to opacities using the same methods as described in § 3.

From the three-dimensional models of the luminosity and dust distributions, a predicted map of the  $2.4 \mu\text{m}$  emission was computed by integrating along the line of sight just as in § 3. Figure 5 compares the predicted map with the observations from Paper I. Clearly, the model does an excellent job of reproducing all the major features in the  $2.4 \mu\text{m}$  map, even to the extent of reproducing many of the subtle wiggles in the contour lines. Figure 6 compares cuts averaged over  $b = \pm 1^\circ$  along the galactic equator from both maps. The free parameters in the model were adjusted to make the two cuts agree with each other on average. However, the location and amplitude of the fluctuations, particularly in the range  $10^\circ < l < 35^\circ$ , depend only on the correctness of the dust model. The predicted fluctuations match the observations quite closely. The largest discrepancy between the model and the data, near  $l = 23^\circ$ , can be attributed to a very large molecular complex, with a mass of  $\approx 5 \times 10^6 M_\odot$ , which is known to lie at the far kinematic distance in that direction (Dame et al. 1986). The significance of this agreement should not be underemphasized: we are testing the calibration of the dust/gas ratio in regions where the opacity is  $\sim 10$  times higher than that where the calibration was established. Given the crudeness of our model for the dust distribution, we choose not to quote any improved value for the dust/gas ratio, but simply note that standard values appear to be entirely satisfactory.

Figure 7 compares the radial light distribution of our "thin" disk with the radial distribution of CO in the Northern hemisphere. The light distribution is considerably narrower than that of the CO, and it peaks at a radius 0.5 kpc inside that of the CO. This offset appears to be real, as we were unable to

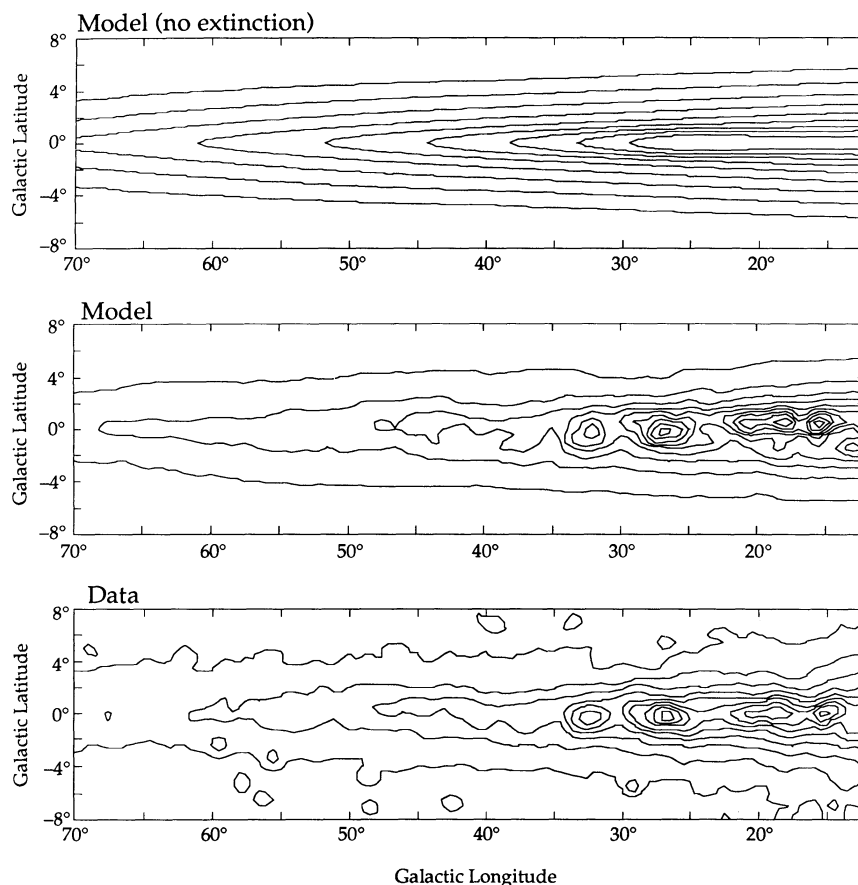


FIG. 5.—*Top*: contour plot of the  $2.4\ \mu\text{m}$  emissivity model including a “thin disk” component but *without* dust extinction. *Middle*: same model as in the top panel but with a three-dimensional dust extinction model included. *Bottom*: contour plot of the Galactic  $2.4\ \mu\text{m}$  emission as mapped by the IRT experiment. In the bottom two panels, the contours are spaced uniformly by the flux corresponding to a surface brightness of  $18.2\ \text{mag arcsec}^{-2}$ .

generate an acceptable model if the two distributions were forced to coincide with each other.

#### 5. COMPARISON WITH OTHER WORK

Estimates of the exponential scale length of the Galaxy have been derived by numerous workers and span an enormous

range: 1.8 to 6 kpc! Table 2 presents a compendium of several recent determinations. Previous estimates based on near-IR observations of stars counts or diffuse integrated emission in the Galactic plane (e.g., Maihara et al. 1978; Jones et al. 1981; Eaton et al. 1984) favor short scale lengths ( $h_R \leq 3\ \text{kpc}$ ). de Vaucouleurs & Pence (1978) derived a value of 3.5 kpc by

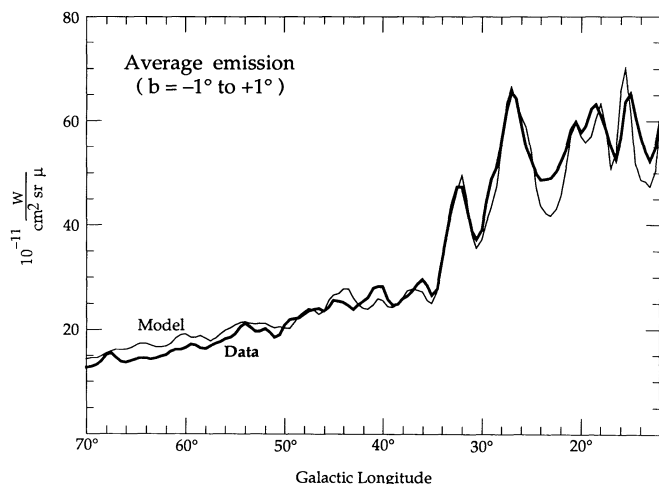


FIG. 6.—Comparison of the observed  $2.4\ \mu\text{m}$  emission in the Galactic plane (*thick line*) and that predicted by the model shown in Fig. 5 (*thin line*). Both profiles are an average of the latitude interval  $-1^\circ < b < 1^\circ$ .

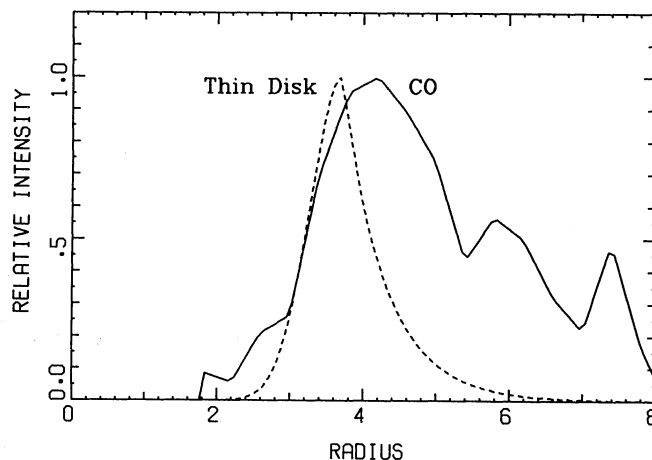


FIG. 7.—Comparison of the radial distribution of CO and excess  $2.4\ \mu\text{m}$  emission in the “thin disk” component. The offset in radius of the peaks is significant.

TABLE 2  
MILKY WAY RADIAL SCALE LENGTH

$h_R$ (kpc)	Technique	Reference
1.8 .....	2.4 $\mu$ m integrated light	1
2.0 .....	2.2 $\mu$ m star counts	2
3.0 .....	2.2 $\mu$ m star counts	3
3.0 $\pm$ 0.5 .....	2.4 $\mu$ m integrated light	4
3.5 .....	B-band comparison with External galaxies	5
4.2 .....	IRAS OH/IR stars	6
4.4 $\pm$ 0.3 .....	Kinematics of disk K giants	7
5.5 $\pm$ 1.0 .....	Pioneer 10 Optical Integrated Light	8
6.0 .....	IRAS OH/IR stars	9

REFERENCES.—(1) Mahara et al. 1978; (2) Jones et al. 1981; (3) Eaton, Adams, & Giles 1984; (4) this paper; (5) de Vaucouleurs & Pence 1978; (6) Habing 1988; (7) Lewis & Freeman 1989; (8) van der Kruit 1986; (9) Rowan-Robinson & Chester 1987.

indirect means. They estimated the local vertically integrated surface brightness of the Galactic disk from star-count data and, by comparison with external galaxies, assumed that the Milky Way disk has a blue central surface brightness of 21.65 mag arcsec<sup>-2</sup>. Lewis & Freeman (1989) deduced a value of 4.4 kpc from observations of the variation in velocity dispersion of disk K-giants with Galactic radius and assuming that  $\sigma \propto \exp(-R/2h)$ . van der Kruit (1986) found a value of 5.5 kpc from the *Pioneer 10* Background Experiment, which measured the longitudinal variation in the integrated starlight in blue and red optical bands at latitudes  $|b| > 20^\circ$  (this value assumes a value for the vertical scale height of the old disk of 325 pc.) Habing (1988) and Rowan-Robinson & Chester (1987) studied the distribution of OH/IR stars discovered by *IRAS*.

Clearly, the measured scale lengths differ by much more than their formal errors. The value of 3 kpc derived here is toward the low end of the estimates listed in Table 2. Why are they so different? A complete discussion will not be attempted here, but some guesses will be offered. First, all measurements require some hidden assumptions (e.g., a dust model or a dynamical model) which may not be valid. van der Kruit's method is sensitive only to the local surface brightness gradient and hence properly measures only the local exponential scale length. Habing (1988) also excludes stars closer than  $2^\circ$  to the Galactic equator. Maihara et al.'s (1978) model gives the scale length for the volume emissivity of an oblate spheroidal model with a fixed ellipticity which is not directly comparable to the other exponential disk models. Lewis & Freeman's (1989) measurement assumes that the velocity dispersion of disk stars is constant with height above the Galactic plane, that the scale height is constant with radius, and that the velocity anisotropy is constant with radius. However, if the distribution of stars perpendicular to the plane is exponential, then the first assumption is wrong (van der Kruit 1988). Finally, different components of the galaxy have different radial distributions, and so one does not expect all scale length measures to be the same. For example, combined optical/infrared studies of external galaxies show that the scale length in the infrared is typically 0.85 times that measured in the optical (Giovanardi & Hunt 1988).

The IRT experiment has two major advantages compared with previous methods: it covers a larger range of Galactic longitude and latitude than other near-IR experiments (with the exception of Hayakawa 1981), and it includes data in the

Galactic plane, where one has the greatest sensitivity to the global radial structure. For studying the distribution of the total stellar mass in the disk, the IRT experiment also has the advantages that it is measuring the distribution primarily of old disk K and M giants and is (hopefully) insensitive to young stars, metallicity gradients, etc. A major uncertainty in interpreting the data is in knowing what fraction of the 2.4  $\mu$ m light comes from M supergiants associated with regions of active star formation. Although our 2.4  $\mu$ m map shows no emission from well-known, nearby H II regions, the "hump" of emission at 4 kpc does coincide with the peak in molecular cloud density, and it has been interpreted by Sera, Puget, & Ryter (1980), Okuda (1981), and Kawara et al. (1982) as arising from a region of active star formation where the luminosity function is different from that of the solar neighborhood. If so, one would expect to see similar enhancements in 2  $\mu$ m images of external galaxies.

Our best-fitting model has a vertical scale height which increases linearly with radius outside  $\sim 5$  kpc. The scale height variation would be even more dramatic had we included the 4 kpc emission hump in our model (Okuda 1981). This result is at variance with the findings of van der Kruit & Searle (1981), who find that the scale height is constant with radius in external edge-on galaxies. The major reason for believing that the variation is real is not that the overall model provides a significantly better fit to our data, but rather that the derived scale height for the fixed-height case is only 204 pc, rather smaller than what is measured for giants in the solar neighborhood. One possible explanation for the discrepancy is that van der Kruit and Searle confined their observations of galactic disks to distances well away from the plane (where dust absorption dominates), and so they are presumably measuring the scale height of old disk stars of high vertical velocity dispersion rather than young stars of low dispersion. Our data make no distinction between old and young stars, and so if the ratio of young/old stars increases toward the Galactic center, then we would incorporate that into our model as a decreasing scale height. Alternatively, van der Kruit and Searle did note that the disks in their sample show signs of flaring (i.e., increasing scale height) toward their edges, and it is possible that the Sun is locating in such a region of flaring in the Milky Way. In either case infrared imaging of external edge-on galaxies will provide more information on the subject.

## 6. COMPARISON WITH THE BULGE AS SEEN BY *IRAS*

Virtually all the mid- and far-infrared emission detected by *IRAS* comes from heated dust in the interstellar medium not directly associated with any stars, and hence a comparison of the 2.4  $\mu$ m map with the equivalent *IRAS* integrated flux maps would not be particularly informative. However, Habing et al. (1985) showed that dust-shrouded asymptotic giant branch stars could be identified in the *IRAS* point source catalog on the basis of their 12  $\mu$ m/25  $\mu$ m color, and these stars also trace the large-scale structure of the Galaxy. Because of sensitivity limits, *IRAS* does not detect all such stars; e.g., Rowan-Robinson & Chester (1987) estimate that half the 12  $\mu$ m flux from stars in the bulge comes from sources not detected by *IRAS*. Nevertheless, some useful comparisons with the 2.4  $\mu$ m data are possible, particularly in the bulge, where problems with incompleteness are reduced.

The structure of the bulge as seen by *IRAS* has been discussed by Harmon & Gilmore (1988). After performing a crude



subtraction of disk sources, they find that the bulge has an ellipticity  $\epsilon_B < 0.3$ , although they are unable to give an accurate value, and that the minor axis profile has an approximately exponential profile with a scale length  $h_B = 375$  pc. Because of problems with source confusion, they only examined data from  $|b| > 4^\circ$ . The upper limit on the bulge ellipticity is smaller than our preferred value of 0.39; however, Harmon and Gilmore may have oversubtracted the disk contribution which would have lead them to find a smaller ellipticity. The exponential falloff in density along the minor axis is in agreement with our assessment of the shape of the bulge profile, and the scale length of 375 pc is close to our best estimate of 407 pc. Even the isophote shapes show some correspondence; e.g., the *IRAS* bulge contours have a "boxy" shape. In short, the *IRAS* view of the bulge matches that of seen at  $2.4 \mu\text{m}$  quite well, even though the types of stars seen at each wavelength are different.

Rowan-Robinson & Chester (1987) estimated the total flux at  $12 \mu\text{m}$  from AGB stars in the region  $350^\circ < l < 10^\circ$ ,  $2^\circ < |b| < 10^\circ$  to be  $1.5 \times 10^4$  Jy. Our model predicts a total flux from the bulge component only of  $2.8 \times 10^5$  Jy, giving a flux ratio  $f_{\nu}(2.2)/f_{\nu}(12) = 19$ . From data in Soifer et al. (1986), Kent (1987), and Persson et al. (1980), we find that the corresponding ratio for the bulge of M31 measured in an aperture of radius  $4'$  is 8.5, only half as large. Thermal emission from dust may already be contributing in this aperture at  $12 \mu\text{m}$ , which would lower the ratio. A more appropriate comparison might be with a dust-free elliptical galaxy. From data in Knapp

(1989), Kent (1987), and Frogel et al. (1978) for the dwarf elliptical M32, we find  $f_{\nu}(2.2)/f_{\nu}(12) = 14$ ; for the giant elliptical NGC 4472, we estimate an even higher value of 36. Given the uncertainties involved, we find that the near-mid infrared spectrum of the Milky Way bulge stars is typical of that other old stellar populations.

## 7. CONCLUSIONS

We have used observations of the diffuse  $2.4 \mu\text{m}$  emission from the northern Galactic plane to model the spatial distribution of  $2.4 \mu\text{m}$  emissivity in the Galaxy. We find that the disk has a radial scale length of 3 kpc and that the vertical exponential scale height may vary with radius but is  $\sim 200$ – $250$  pc in the solar neighborhood. If the bulge is modeled as an oblate spheroid with an exponential profile, then the minor axis scale length is 407 pc and the ellipticity is 0.39. The ratio of bulge/disk light is 1:5.

We have shown that fine structure in the map of  $2.4 \mu\text{m}$  emission can be explained almost entirely as being due to variations in interstellar extinction along the line of sight. The amplitude of the intensity fluctuations agree close with those predicted using standard values for the dust/gas ratio, even though we are probing optical depths 10 times larger than those where the calibration was made.

This work has been supported by NASA contract NAS8-32845 and NSF grant AST 8451724.

## REFERENCES

- Bahcall, J. H., & Soneira, R. M. 1980, *ApJS*, 44, 73  
 Barker, P. L., & Burton, W. B. 1978, *ApJ*, 281, 97  
 Becklin, E. E., & Neugebauer, G. 1968, *ApJ*, 151, 145  
 Bohlin, R. C., Savage, B. D., & Drake, J. F. 1978, *ApJ*, 224, 132  
 Bronfman, L., Cohen, R. S., Alvarez, H., May, J., & Thaddeus, P. 1988, *ApJ*, 324, 248  
 Burton, W. B. 1988, in *Galactic and Extragalactic Radio Astronomy*, ed. G. L. Verschuur and K. I. Kellerman (Berlin, Springer-Verlag), p. 332  
 Caldwell, J., & Ostriker, J. 1981, *ApJ*, 251, 61  
 Dame, T. M., Elmegreen, B. G., Cohen, R. S., & Thaddeus, P. 1986, *ApJ*, 305, 892  
 Dame, T. M., Ungerechts, H., Cohen, R. S., de Geus, E. J., Grenier, I. A., May, J., Murphy, D. C., Nyman, L.-A., & Thaddeus, P. 1987, *ApJ*, 322, 706  
 de Vaucouleurs, G., & Pence, W. D. 1978, *AJ*, 83, 1163  
 Eaton, N., Adams, D. J., & Giles, A. B. 1984, *MNRAS*, 208, 241  
 Frankston, M., & Schild, R. 1976, *AJ*, 81, 500  
 Frogel, J. A., Persson, S. E., Aaronson, M., & Mathews, K. 1978, *ApJ*, 220, 75  
 Garwood, R., & Jones, T. 1987, *PASP*, 99, 453  
 Gilmore, G., & Reid, I. N. 1983, *MNRAS*, 202, 1025  
 Giovanardi, C., & Hunt, L. K. 1988, *AJ*, 95, 408  
 Grabelsky, D. A., Cohen, R. S., Bronfman, L., Thaddeus, P., & May, J. 1987, *ApJ*, 315, 122  
 Habing, H. J. 1988, *A&A*, 200, 40  
 Habing, H. J., Olmon, F. M., Chester, T., Gillett, F., Rowan-Robinson, M., & Neugebauer, G. 1985, *A&A*, 152, L1  
 Harmon, R., & Gilmore, G. 1988, *MNRAS*, 235, 1025  
 Hayakawa, S., Ito, K., Matsumoto, T., & Uyama, K. 1977, *A&A*, 58, 325  
 Hayakawa, S., Matsumoto, T., Murakami, H., Uyama, K., Thomas, J. A., & Yamagami, T. 1981, *A&A*, 100, 116  
 Ishida, K., & Mikami, T. 1982, *PASJ*, 34, 89  
 Ito, K., Matsumoto, T., & Uyama, K. 1976, *PASJ*, 28, 427  
 Jarvis, B. J. 1986, *AJ*, 91, 65  
 Jones, T. J., Ashley, M., Hyland, A. R., & Ruelas-Mayorga, A. 1981, *MNRAS*, 197, 413  
 Kawara, K., Kozasa, T., Sato, S., Kobayashi, Y., & Okuda, H. 1982, *PASJ*, 34, 389  
 Kent, S. M. 1987, *AJ*, 94, 306  
 Kent, S. M., Mink, D., Fazio, G. D., Melnick, G., Tardiff, A., & Maxson, C. 1991, *ApJ*, submitted (Paper I)  
 Knapp, G. R., Guhathakurta, P., Kim, D.-W., & Jura, M. 1989, *ApJS*, 70, 329  
 Koch, D., Fazio, G. G., Traub, W. A., Rieke, G. H., Gautier, T. N., Hoffman, W. F., Low, F. J., Poteet, W., Young, E. T., Urban, E. W., & Katz, L. 1982, *Optical Eng.*, 21, 141  
 Kormendy, J. 1980, in *Proc. 12th Advanced Course of the Swiss Society of Astronomy and Astrophysics*, (Sauverny: Geneva Observatory), p. 144  
 Lewis, J. R., & Freeman, K. C. 1989, *ApJ*, 97, 139  
 Lockman, F. J. 1984, *ApJ*, 283, 90  
 Maihara, T., Oda, N., Sugiyama, T., & Okuda, H. 1978, *PASJ*, 30, 1  
 Melnick, G. J., Fazio, G. G., Koch, D. G., Rieke, G. H., Young, E. T., Low, F. J., Hoffman, W. F., & Gautier, T. N. 1987, *AIP Conf. Proc.* 155, The Galactic Center, ed. D. C. Backer (New York: AIP), p. 157  
 Oda, N. 1985, *A&A*, 145, 45  
 Oda, N., Maihara, T., Sugiyama, T., & Okuda, H. 1979, 72, *A&A*, 309  
 Okuda, H. 1981, in *IAU Symposium 96, Infrared Astronomy*, ed. C. G. Wynn-Williams & D. P. Cruikshank (Dordrecht: Reidel), p. 247  
 Persson, S. E., Cohen, J. G., Sellgren, K., Mould, J. R., & Frogel, J. 1980, *ApJ*, 240, 779  
 Pritchett, C. 1983, *AJ*, 88, 1476  
 Reid, M. J. 1989, in *IAU Symposium 136, The Center of the Galaxy*, ed. M. Morris (Dordrecht: Kluwer Academic) p. 37  
 Rieke, G., & Lebofsky, M. 1985, *ApJ*, 288, 618  
 Rowan-Robinson, M., & Chester, T. 1987, *ApJ*, 313, 413  
 Schwarzschild, B. 1990, *Physics Today*, 43, No. 7, 19  
 Sera, G., Puget, J. L., & Ryter, C. E. 1980, *A&A*, 84, 220  
 Soifer, B. T., Rice, W. L., Mould, J. R., Gillett, F. C., Rowan-Robinson, M., & Habing, H. J. 1986, *ApJ*, 304, 651  
 Strong, A. W., et al. 1988, *A&A*, 207, 1  
 van der Kruit, P. C. 1986, *A&A*, 157, 230  
 ———. 1988, *A&A*, 192, 117  
 van der Kruit, P. C., & Searle, L. 1981, *A&A*, 95, 105  
 Wainscoat, R. J., Freeman, K. C., & Hyland, A. R. 1989, *ApJ*, 337, 163  
 Weaver, H., & Williams, D. R. W. 1973, *A&AS*, 8, 7